[3]Anon., *Naval Test Pilot School Flight Test Manual—Fixed Wing Stability and Control, Theory and Flight Test Techniques*, Naval Air Warfare Center, Aircraft Div., USNTPS-FTM 103, Patuxent River, MD, revised Aug. 1977.
[4]Etkin, B., *Dynamics of Flight—Stability and Control*, 2nd ed., Wiley, Toronto, Canada, 1982.
[5]Nelson, R. C., *Flight Stability and Automatic Control*, McGraw-Hill, New York, 1989.
[6]Raymer, D. P., *Aircraft Design: A Conceptual Approach*, 1st ed., AIAA, Washington, DC, 1989.
[7]Solies, U. P., "Effects of Thrust Line Offset on Neutral Point Determination in Flight Testing," *Journal of Aircraft*, Vol. 31, No. 2, March-April 1994, pp. 362–366.

Passive Porosity with Free and Fixed Separation on a Tangent-Ogive Forebody

Richard M. Wood,* Daniel W. Banks,† and Steven X. S. Bauer‡
NASA Langley Research Center, Hampton, Virginia 23665

Nomenclature

C_N = normal force coefficient
C_Y = side force coefficient
α = angle of attack, deg

Introduction

THE passive porosity concept has been extensively studied both experimentally and computationally as a means to control shock/boundary-layer interaction[1-5] and to control flow separation in a weapons bay cavity.[6] The present focus of passive porosity at the National Aeronautics and Space Administration, Langley Research Center is the global application of passive porosity on an aerodynamic vehicle to control the forces and moments of the vehicle.

As a first step in assessing the global application of passive porosity, a review of the literature was conducted that identified high alpha forebody aerodynamics as being of high interest to the aerodynamic community.[7] Experimental data show that slender forebodies at zero sideslip can exhibit large asymmetric loadings about the vertical plane of symmetry at moderate to large angles of attack.[8,9] The character of these asymmetric loads has also been shown to vary with Mach number and boundary-layer state.[7-10] Various experimental studies have been conducted to investigate aerodynamic control effector concepts that control or eliminate the asymmetric loading on slender axisymmetric bodies by controlling the extent of attached flow about the side of the bodies.[11,12] In a recent study by Bauer,[13] passive porosity was successfully employed on a slender axisymmetric forebody to eliminate the loading asymmetry typically observed at moderate to high angles of attack and zero sideslip. The work of Bauer is the first application of passive porosity to control the global pressure loading on a three-dimensional geometry.

Despite the extensive experimental and computational data base within the literature on passive porosity, there is no clear explanation of the governing flow physics. It is theorized that the passive porosity concept modifies the external pressure loading by allowing communication between high- and low-pressure regions on the external surface. One phenomena associated with the communication between high- and low-pressure regions is a minimal transfer of air into the internal chamber at the high-pressure region, and out of the internal chamber at the low-pressure region.[1-4] The second phenomena that may occur is a direct pressure communication between high- and low-pressure regions on the exterior surfaces of the member (i.e., standing pressure wave). Of primary concern within the present research program is determining the dominant flow phenomena that govern the effectiveness of passive porosity (modify forces) with respect to each application.

The present research effort is directed at assessing the contribution of each phenomena as related to a porous slender axisymmetric forebody. To assess the influence of the mass transfer and pressure equalization phenomena to the effectiveness of passive porosity on slender axisymmetric forebodies, strakes were attached to the 5.0-caliber solid and porous forebodies of Ref. 12 to force crossflow separation. The tests were conducted in the NASA Langley Research Center 14- by 22-ft Subsonic Wind Tunnel.[14] Longitudinal force and moment data were obtained at a Mach number of 0.1 over an angle-of-attack range of 0 to 55 deg.

Model Description

The solid and porous wind-tunnel models were 5.0-caliber tangent-ogive with a 2.5-diam (10-in.) cylindrical extension. The models were 30 in. long and had a base diameter of 4 in. The solid and porous models consist of shells of minimum wall thickness that fit over a common centerbody/balance housing. The centerbody, to which the solid and porous shells were attached, is 30 in. long with a maximum diameter of 2.5 in. The region between the o.d. of the centerbody and the i.d. of the forebody shell was used as the plenum for the porous forebody test.

The porous forebody model had a surface porosity of 22% on the 5.0-caliber tangent-ogive section, and had surface porosity that varied linearly from 22 to 0% from the end of the tangent-ogive section to half the length of the cylindrical extension. The rear half of the cylindrical extension was solid. Surface porosity was created by drilling equally spaced (based upon the desired porosity value) 0.020-in.-diam holes over the surface.

As shown in Fig. 1, both large and small strakes attached to the forebody models at the 85- and 265-deg circumferential positions, referenced to the model bottom centerline, and viewed looking forward. The left to right (85 and 265 deg) strake asymmetry was created to induce a unidirectional side force that could be investigated with passive porosity. The

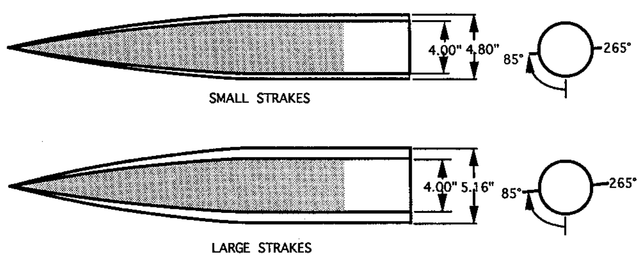

Fig. 1 Sketch showing details of the small and large strakes.

Presented as Paper 92-4494 at the AIAA Atmospheric Flight Mechanics Conference, Hilton Head, SC, Aug. 10–12, 1992; received March 8, 1993; revision received Oct. 29, 1993; accepted for publication Oct. 30, 1993. Copyright © 1993 by the American Institute of Aeronautics and Astronautics, Inc. No copyright is asserted in the United States under Title 17, U.S. Code. The U.S. Government has a royalty-free license to exercise all rights under the copyright claimed herein for Governmental purposes. All other rights are reserved by the copyright owner.

*Assistant Head, High Reynolds Number Aerodynamics Branch.
†Senior Research Engineer, Subsonic Aerodynamics Branch.
‡Senior Research Engineer, Supersonic/Hypersonic Aerodynamics Branch.

small and large strakes extended the full length of the forebodies and have a local semispan of 20 and 40% of the local body diameter, respectively.

Test and Instrumentation

The test was conducted in the NASA Langley Research Center 14- by 22-ft Subsonic Wind Tunnel at a Mach number of 0.1 and a unit Reynolds number of 1×10^6/ft. To represent the surface roughness of the porous body, the solid body was tested with boundary-layer transition grit applied over the entire surface, 1 in. aft of the fuselage nose. The grit size and location was based upon the data of Ref. 14.

Longitudinal force and moment data were obtained at angles of attack from 0 to 55 deg. The data were measured with a six-component strain-gauge balance mounted in the centerbody and connected by a sting to the tunnel permanent model actuation system.

Balance chamber, model base, and vent chamber pressures were obtained throughout the test. The balance chamber and model base pressures were used to correct the force and moment data to freestream conditions at the model base. The vent-chamber pressures were obtained to assess the passive porosity physics.

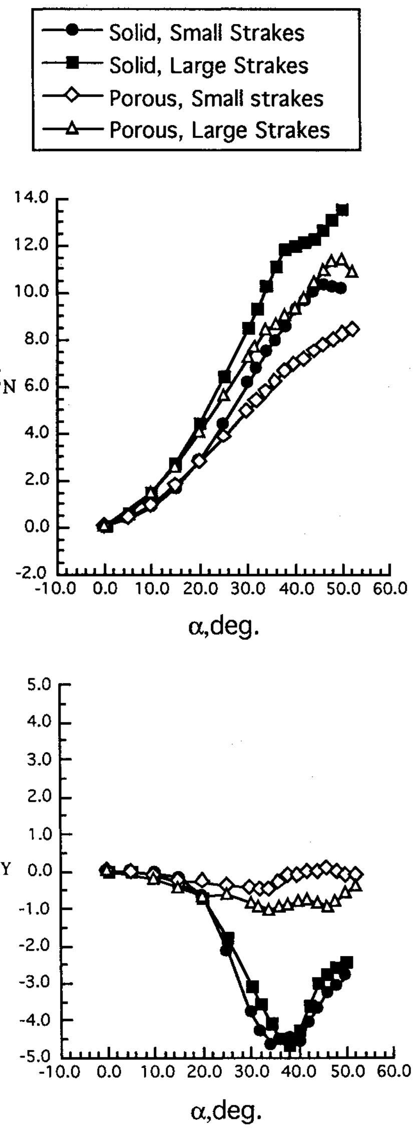

Fig. 2 Effect of fixed and free crossflow separation on the normal force and side force characteristics for the solid and porous 5.0-caliber forebodies.

Discussion

Six-component force and moment data were obtained on the porous and solid 5.0-caliber tangent-ogive forebody models both with and without the small and large strakes. However, only the normal force and side force characteristics will be discussed in this Note. The data obtained for the porous forebody model was obtained without boundary-layer transition grit.

Presented in Fig. 2 are normal force and side force coefficient data for the solid and porous forebody models with the large and small strakes. The normal force coefficient data of Fig. 2 show that porosity significantly reduces the normal force from that for the solid body. The reduced normal force for the porous surface forebodies, compared to the solid forebody with strakes, is most likely due to an increase in the upper surface pressures caused by the communication between the high- and the low-pressure regions on the porous surface. The side force coefficient data of Fig. 2 show that passive porosity is effective at eliminating the induced asymmetric loading on the forebody with strakes. The slight residual side force increment remaining for the porous forebody with strakes may be attributed to the loading on the asymmetric strakes and not the loading on the porous surface. These data suggest that direct pressure equalization and not the mass transfer effect is dominating the effectiveness of passive porosity for the forebody with strakes.

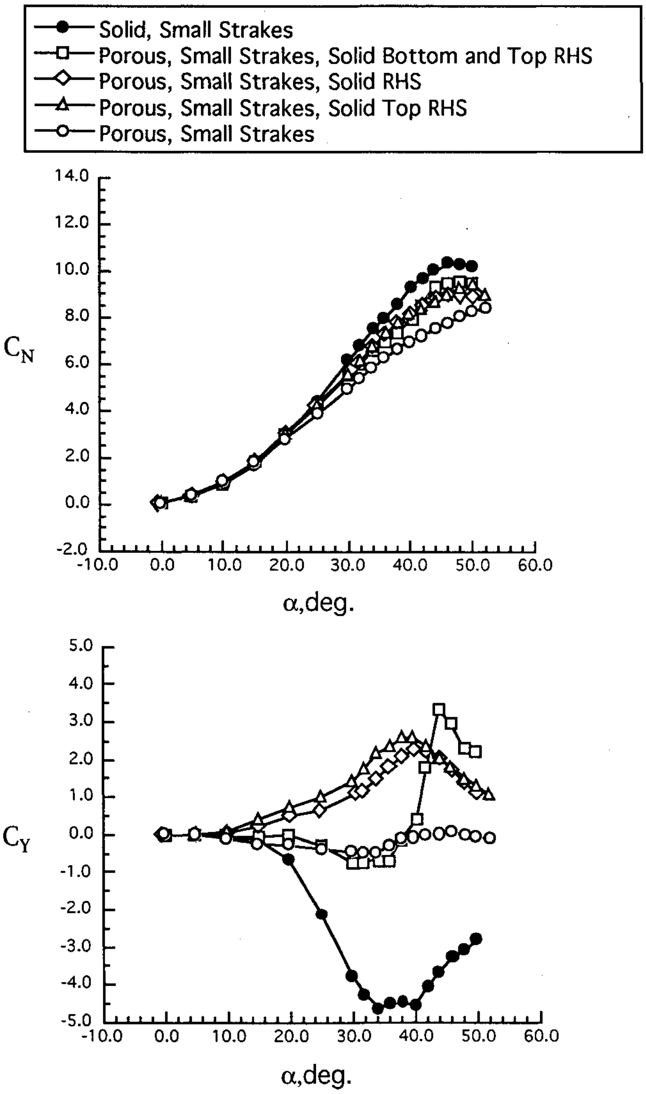

Fig. 3 Effect of the circumferential extent of porosity on the normal force and side force characteristics of the 5.0-caliber forebody with small strakes.

To further evaluate the direct pressure communication effect, the porous forebody with small strakes was configured by covering various regions of the porous surface with tape in order to create a local solid region on the porous forebody. The surface that has been taped over will be referred to as solid. The normal force and side force characteristics of several geometries are presented in Fig. 3.

Data are presented in Fig. 3 for the porous, solid upper right quadrant, solid right side, solid upper right quadrant with solid bottom, and the solid with the small strakes. The normal force data show that a solid top right quadrant contributes approximately one-half of the increment in normal force between the porous and solid forebodies with small strakes. The data show that a porous lower surface significantly influences the effectiveness of passive porosity to alleviate the asymmetric loading on the upper surface. The side force data show that upper surface passive porosity in combination with lower surface passive porosity provides improved effectiveness over upper surface passive porosity alone. This is especially evident for the configuration with a solid lower surface and solid top right quadrant.

Concluding Remarks

An experimental investigation to assess the effectiveness of passive porosity to change the pressure loading with free and fixed crossflow separation was conducted on a 5.0-caliber tangent-ogive forebody in the NASA Langley Research Center 14- by 22-ft Subsonic Wind Tunnel. The data show that the effectiveness of passive porosity to modify the forces for forced crossflow separation conditions is similar to that observed for the free crossflow separation condition. The data also show that the effectiveness of passive porosity to change the forces is significantly enhanced with the presence of large positive pressures on the porous surface. A preliminary look at the effect of plenum geometry showed that the effectiveness of the passive porosity system can be degraded if communication between high- and low-pressure regions is restricted.

References

[1]Nagamatsu, H. T., and Orozco, R. D., "Porosity Effect on Supercritical Airfoil Drag Reduction by Shock Wave Boundary Layer Control," AIAA Paper 84-1682, June 1984.

[2]Theide, P., Krogmann, P., and Syanewsky, E., "Active and Passive Shock/Boundary Layer Interaction Control on Supercritical Airfoils," AGARD-CP-365, 1984.

[3]Bahi, L., and Ross, J. M., "Passive Shock Wave/Boundary Layer Control for Transonic Airfoil Drag Reduction," AIAA Paper 83-0137, Jan. 1983.

[4]Chen, C.-L., Chow, C.-Y., Van Dalsem, W., and Holst, T., "Computation of Viscous Transonic Flow over Porous Airfoils," AIAA Paper 87-0359, July 1987.

[5]Olling, C. R., and Dulikravich, G. S., "Porous Airfoils Analysis Using Viscous-Inviscid Coupling at Transonic Speeds," *International Journal of Numerical Methods in Fluids*, Vol. 7, Feb. 1987, pp. 103–109.

[6]Wilcox, F. J., "Experimental Investigation of the Effects of a Porous Floor on Cavity Flow Fields at Supersonic Speeds," NASA TP 3032, March 1990.

[7]Hall, R. M., Erickson, G. E., Banks, D. W., and Fisher, D. F., NASA High Angle of Attack Technology Conf., Hampton, VA, Oct.–Nov. 1990.

[8]Allen, H. J., and Perkins, E. W., "A Study of the Effects of Viscosity on Flow over Slender Inclined Bodies of Revolution," NACA TR 1048, 1951.

[9]Letko, W., "A Low-Speed Experimental Study of the Directional Characteristics of a Sharp Nosed Fuselage Through a Large Angle of Attack Range at Zero Angle of Sideslip," NACA TN 2911, 1953.

[10]Coe, P. L., Jr., Chambers, J. R., and Letko, W., "Asymmetric Lateral-Directional Characteristics of Pointed Bodies of Revolution at High Angles of Attack," NASA TN D-7095, 1973.

[11]Jorgensen, L. H., and Nelson, E. R., "Experimental Aerodynamic Characteristics for a Cylindrical Body of Revolution with Various Noses at Angles of Attack from 0° to 58° and Mach Numbers from 0.6 to 2.0," NASA TM X-3128, 1974.

[12]Jorgensen, L. H., and Nelson, E. R., "Experimental Aerodynamic Characteristics for a Cylindrical Body of Revolution with Side Strakes and Various Noses at Angles of Attack from 0° to 58° and Mach Numbers from 0.6 to 2.0," NASA TM X-3130, March 1975.

[13]Bauer, S. X. S., and Hemsch, M. J., "Alleviation of Side Force on Tangent Ogive Forebodies Using Passive Porosity," AIAA Paper 92-2711, June 1992.

[14]Gentry, G. L., Jr., Quinto, P. F., Gatlin, G. M., and Applin, Z. T., "The Langley 14- by 22-Foot Subsonic Tunnel: Description, Flow Characteristics, and Guide for Users," NASA TP-3008, Sept. 1990.

Vortical Flow Structure near the F/A-18 LEX at High Incidence

B. H. K. Lee* and N. R. Valerio†
Institute for Aerospace Research,
Ottawa, Ontario K1A 0R6, Canada

Introduction

THE high degree of maneuverability of the F/A-18 at subsonic flight speeds is largely credited to the leading-edge extension (LEX) that generates large nonlinear lift at high angles of attack. The lift enhancement arises from vortex generated by the rolling-up of separated flow at the highly swept leading edge of the LEX. Ultimately, the two LEX vortices burst and the resulting turbulent flow impacts on the tail section of the aircraft causing severe structural damage.[1] Some alleviation of the loads on the aircraft horizontal stabilizers and vertical fins can be achieved by the installation of a streamwise fence on the LEX.[2] The role of the fence is to alter the flow structure of the LEX vortices.

Flow visualization studies[3,4] of the flow in the vicinity of the F/A-18 LEX show a pair of corotating vortices emerging downstream of the fence. However, a mechanism explaining the presence of these vortices is not elucidated in Refs. 3 and 4 due to limitations in the experimental techniques used.

This Note attempts to provide further insight into the complex flow structure generated by the LEX and fence through a study of the topology of the surface skin friction lines. The experiment was carried out on a 6% scale rigid model of the F/A-18 in the IAR 1.5-m Trisonic Blowdown Wind Tunnel. Various angles of attack were investigated. The results presented herein are for $M = 0.6$ and $\alpha = 30$ deg.

Model and Experimental Technique

The model is described in detail in Ref. 2. The leading- and trailing-edge flap deflections were set at 34 and 0 deg, respectively. The horizontal stabilizer angle was positioned at -9 deg for the wind-tunnel investigation. Models of the Aim 9 missiles were mounted at the wingtips.

For flow visualization studies, oil dots, formed by mixing SAE 30-grade motor oil with carbon black, were deposited on the upper surface of the LEX and on both surfaces of the

Received Nov. 2, 1993; revision received Nov. 29, 1993; accepted for publication Dec. 3, 1993. Copyright © 1994 by B. H. K. Lee and N. R. Valerio. Published by the American Institute of Aeronautics and Astronautics, Inc., with permission.

*Senior Research Officer, National Research Council, High Speed Aerodynamics Laboratory; also, adjunct Professor, Department of Mechanical Engineering, University of Ottawa, Ottawa, Ontario K1N 6N5, Canada. Associate Fellow AIAA.

†Guest Worker, National Research Council, Department of Mechanical Engineering, McGill University, Montreal, Quebec H3A 2K6, Canada.